

# Sensitization and Tunneling Corrosion of Austenitic Type 347 Stainless Steel

C.A. Teodoro\* and S. Wolyneć\*\*

## ABSTRACT

*Sensitization of type 347 (UNS S34700) austenitic stainless steel (SS) samples removed from forged bars was investigated using the electrochemical potentiokinetic reactivation (EPR) method and the weight-loss technique of ASTM A 262, Practice B. A normal and a low-carbon steel were investigated. After solution-annealing at 1,050°C, the two steels were submitted to sensitization treatments at 550°C, 670°C, 790°C, and 910°C for times varying from 1 h to 130 h. The steel with normal carbon content also was solution-annealed at 1,140°C and submitted to the same sensitization treatments for times varying from 1 h to 62 h. Correlation between results obtained by the two techniques was very poor. The lack of correlation was ascribed to tunneling corrosion, which is typical of forged steels; in addition to intergranular corrosion resulting from sensitization. The electrochemical test was most sensitive to corrosion by sensitization. The Practice B test did not discriminate between the two types of attack. The steel solution-annealed at higher temperature was more susceptible to sensitization.*

**KEY WORDS:** austenitic stainless steel, intergranular corrosion, sensitization, tunneling corrosion, type 347 stainless steel, UNS S34700

Submitted for publication January 1997; in revised form, May 1997.

\* Institute for Energy and Nuclear Research (IPEN/CNEN-SP-REN), Caixa Postal 11.049, 05422-970, São Paulo, SP, Brazil.

\*\* Department of Metallurgical and Materials Engineering, Polytechnic School of the University of São Paulo (PMT/EPUSP), Av. Prof. Mello Moraes, 2463, 05508-900, São Paulo, SP, Brazil.

†† UNS numbers are listed in *Metals and Alloys in the Unified Numbering System*, published by the Society of Automotive Engineers (SAE) and cosponsored by ASTM.

## INTRODUCTION

The austenitic stainless steel (SS) sensitization process, which consists of carbide precipitation at grain boundaries and chromium depletion in adjacent regions and makes the material susceptible to intergranular corrosion, has been investigated thoroughly. The kinetics involve the carbide precipitation process and the chromium diffusion process to regions depleted in this element. The kinetics still present some obscure and controversial points, however, especially in steels such as type 347 SS (UNS S34700).<sup>(1)</sup> This steel contains niobium that is intended to combine preferentially with carbon to prevent chromium carbide precipitation. However, as shown by Padilha for type 321 SS (UNS S32100), to which titanium is added instead of niobium, only a part of the carbon combines with the titanium after the solution-anneal and the rest remains in solution.<sup>1</sup> Moreover, he found that the kinetics of chromium carbide formation, although metastable, is more favorable than that of titanium carbide (TiC) at temperatures < 600°C. Above this temperature, the opposite is true. This explains why these steels become sensitized and susceptible to intergranular corrosion under certain circumstances.

Austenitic SS under forged conditions also may become susceptible to tunneling corrosion, also known as end-grain attack. This corrosion, which has a pitting corrosion morphology, propagates along the metal flows of SS forgings.<sup>2</sup> It has been ascribed to alignment of nonmetallic impurities (sulfides,

12425

TABLE 1  
Chemical Composition of Steels Tested (wt%)

Element	Steel 347	Steel 347L
C	0.064	0.014
Si	0.45	0.45
Mn	1.76	1.79
P	0.005	0.004
S	0.005	0.004
Cr	17.65	17.4
Ni	9.95	9.85
Nb + Ta	0.76	0.39
Fe	69.3	69.7

oxides, etc.) or refractory metal carbides that form preexisting active paths for the corrosion front.<sup>3</sup> In sensitized type 347 SS, submitted to the Huey test, this type of corrosion was shown to follow the niobium carbide (NbC) stringer.<sup>4</sup> However, the phenomenon also has been observed (albeit to a reduced extent) on extra high-purity, low-carbon SS.<sup>3</sup> Kajimura, et al.,<sup>2</sup> detected this type of corrosion for 25% Cr-20% Ni-Nb SS in highly oxidizing nitric acid (HNO<sub>3</sub>) and showed it resulted from chromium segregation, causing chromium depletion in the cold-worked bands parallel to the metal flows from working.

The objective of the present work was to investigate the sensitization of forged type 347 SS samples using an electrochemical potentiokinetic reactivation (EPR) method and the weight-loss technique outlined ASTM A 262, Practice B.<sup>(2)</sup> Use of the EPR technique as a suitable tool for investigating sensitization of these steels and that of type 304 SS (UNS S30400) has been reported elsewhere.<sup>5</sup>

## EXPERIMENTAL

Two different type 347 austenitic SS were investigated. The first, designated as Steel 347, contained normal carbon content, while the second, designated as Steel 347L, contained much lower carbon and niobium contents. Chemical composition of these steels is given in Table 1.

Samples of these steels, removed from forged bars, initially were solution-annealed at 1,050°C for 40 min, followed by quenching in water. Afterward, they were submitted to sensitization treatments at 550°C, 670°C, 790°C, and 910°C for times of 1 h, 13 h, 62 h, and 130 h. Steel 347 also was solution-annealed at 1,140°C for 40 min and then submitted to the same sensitization treatments for times of 1 h, 13 h, and 62 h. Thus, Steel 347 was formed by two sets of samples: the first, corresponding to the

1,050°C solution-annealing temperature, was designated as 347(1) and the other, corresponding to 1,140°C, was designated as 347(2).

The double-loop (DL)-EPR method was used to determine the degree of sensitization (DOS). The experimental setup was assembled as described in the literature.<sup>6,7</sup> A saturated calomel electrode (SCE) and a platinum counter electrode were used in the testing cell, which contained a 0.5 M sulfuric acid (H<sub>2</sub>SO<sub>4</sub>) + 0.01 M potassium thiocyanate (KSCN) solution prepared with analytical-grade reagents. Testing temperature was maintained constant at 30°C ± 1°C, and the scanning rate of the polarization cycle (corrosion potential) → (fixed potential in the passive region) → (corrosion potential) was 2 mV/s. The fixed potential in the passive region was 300 mV<sub>SCE</sub>. In this method, DOS was evaluated with the I<sub>2</sub>/I<sub>1</sub> ratio, where I<sub>1</sub> is the peak current in the polarization cycle (corrosion potential) → (fixed potential in the passive region), and I<sub>2</sub> is the peak current obtained in the reverse cycle (fixed potential in the passive region) → (corrosion potential).

For the sake of comparison, DOS also was determined using the Practice B weight-loss technique of the ASTM A 262 standard; but instead of the specified 120-h testing, 30-min or 40-min tests were performed.

Samples for the DL-EPR test were mounted in thermosetting plastic, leaving an exposed surface area of ~ 1 cm<sup>2</sup> (0.155 in.<sup>2</sup>) that was wet-polished to 600-grade silicon carbide (SiC) paper. Samples for the Practice B test were approximately cubic in shape and had an approximate area of 13 cm<sup>2</sup> (2.015 in.<sup>2</sup>). They were wet-polished in all their faces down to 120-grade SiC paper.

## RESULTS

DL-EPR tests were repeated three times each after polishing, so that each I<sub>2</sub>/I<sub>1</sub> ratio value was the average of three measures. The standard deviation is indicated in the figures by the error bars. Since the Practice B tests were intended only for comparison, they were performed once.

For Steel 347(1), DOS values with heat treatment time at different temperatures are presented in Figure 1 for the DL-EPR test and in Figure 2 for the Practice B test. For the solution-annealed condition (time zero), the I<sub>2</sub>/I<sub>1</sub> ratio for this steel was 0.0019, and the weight loss was 3.1 g/m<sup>2</sup>-h.

According to the DL-EPR tests (Figure 1), Steel 347(1) became sensitized only for the 550°C sensitization treatment. This sensitization also was detected by the Practice B test (Figure 2). However, in comparing the two figures, it was observed that, while no sensitization was detected by the DL-EPR technique for other temperatures, considerable weight loss was determined by Practice B for the sample treated 13 h

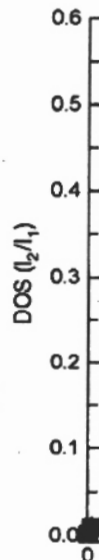


FIGURE 1  
time at diff

at 670°C  
670°C a  
Sin  
347L (P  
dition (0  
0.0032  
DL  
of some  
samples  
B tests  
quite co  
for 1-h  
gible, w  
5,000 g  
670°C a  
substanc  
and neg  
The  
Steel 34  
effect u  
solution  
for Steel  
2.0 g/m  
Cor  
while se  
steel so  
in all te  
1,140°C  
results  
EPR tes  
both w  
sults, th  
than 79

<sup>(2)</sup> ASTM A 262-91, "Practices for Detecting Susceptibility to Intergranular Attack in Austenitic Stainless Steels," vol. 03.02, Annual Book of Standards (West Conshohocken, PA: ASTM, 1991).

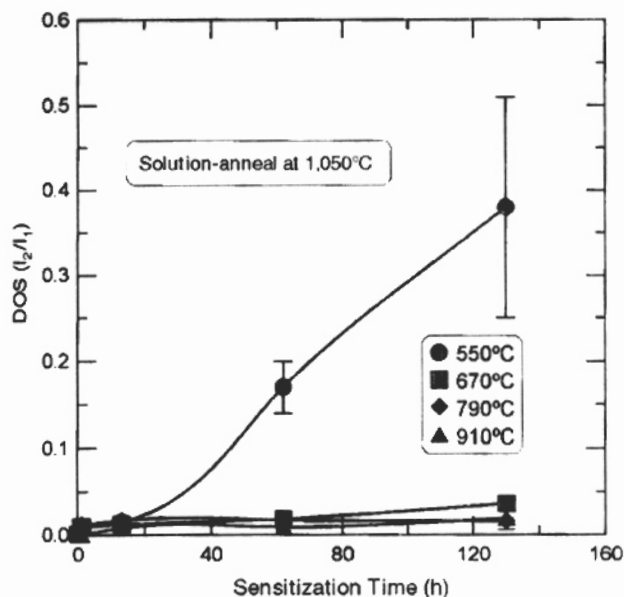


FIGURE 1. DOS variation of Steel 347(1) with sensitization treatment time at different temperatures as determined by the DL-EPR technique.

at 670°C, as well as for samples treated 130 h at 670°C and 910°C.

Similar discrepancies were observed for Steel 347L (Figures 3 and 4). For the solution-anneal condition (time zero), the  $I_2/I_1$  ratio for this steel was 0.0032, and the weight loss was 3.0 g/m<sup>2</sup>-h.

DL-EPR tests (Figure 3) indicated the occurrence of some sensitization of Steel 347L, particularly for samples treated at 790°C and 550°C. In the Practice B tests (Figure 4), the behavior of this steel was quite complex. At 550°C, for example, the weight loss for 1-h and 62-h sensitization treatments was negligible, while for 13 h and 130 h, it was of the order of 5.000 g/m<sup>2</sup>-h and 3.500 g/m<sup>2</sup>-h, respectively. For 670°C and 790°C, however, the weight loss was substantial for 1-h, 62-h, and 130-h treatment, and negligible for 13-h treatment.

The change of solution-annealing temperature of Steel 347 from 1,050°C to 1,140°C had a significant effect upon its sensitization (Figures 5 and 6). For the solution-anneal condition (time zero), the  $I_2/I_1$  ratio for Steel 347(2) was 0.0028, and the weight loss was 2.0 g/m<sup>2</sup>-h.

Comparison of Figure 5 to Figure 1 showed that, while sensitization was only significant at 550°C for steel solution-annealed at 1,050°C, it was meaningful in all temperatures for that solution-annealed at 1,140°C, being more intense at 670°C. Weight-loss results (Figure 6) showed some agreement with DL-EPR tests results (Figure 5) for 670°C and for 790°C, both with a maximum at 13 h. In the DL-EPR results, this maximum was ~ 3 times larger for 670°C than 790°C. In the weight-loss results, the 670°C

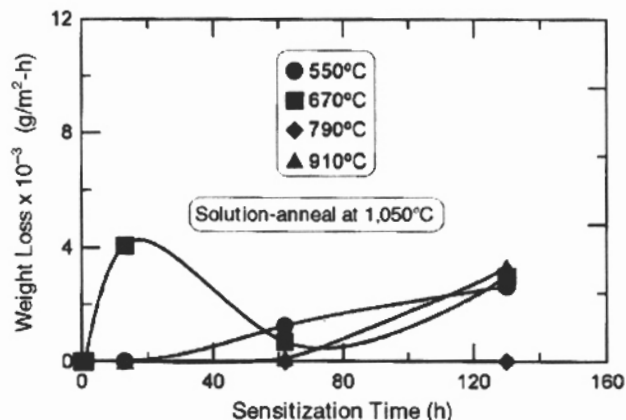


FIGURE 2. Weight-loss variation of Steel 347(1) with sensitization treatment time at different temperatures as determined using ASTM A 262, Practice B, after 40 min of immersion.

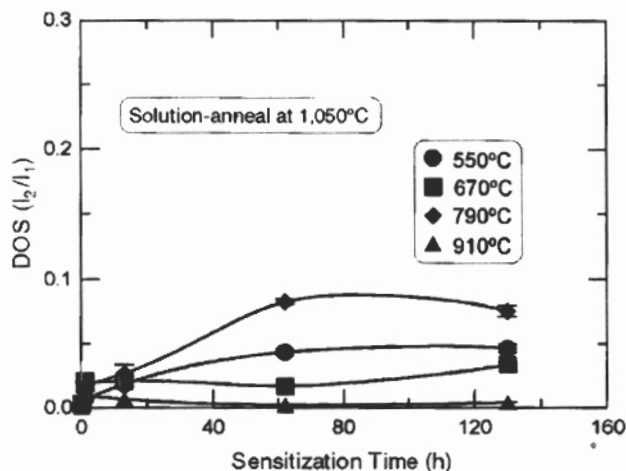


FIGURE 3. DOS variation of Steel 347L with sensitization treatment time at different temperatures as determined by the DL-EPR technique.

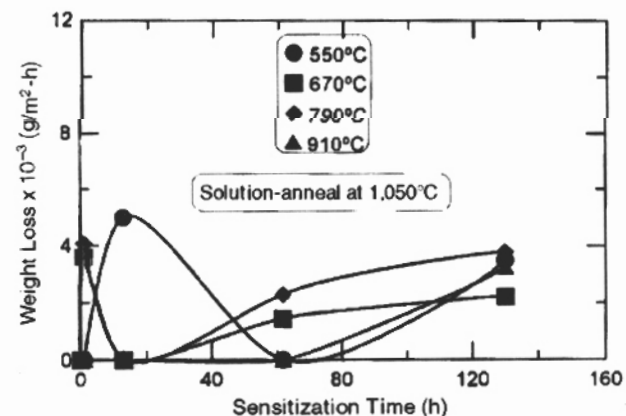


FIGURE 4. Weight-loss variation of Steel 347L with sensitization treatment time at different temperatures as determined using ASTM A 262, Practice B, after 40 min of immersion.

desig-  
to

ped to  
the ex-  
l in the  
(E) and  
testing  
SO<sub>4</sub>) +  
in pre-

± 1°C,  
e (corro-  
re  
the fixed  
: In this  
to,  
n cycle  
passive  
the  
gion) →

is deter-  
que of  
speci-  
re

ed in  
face  
shed to  
es for  
in shape  
5 in.?)  
n to

each  
was the  
tation is  
ice the  
arison,

reatment  
in Fig-  
the  
ndition  
0019.

, Steel  
sensi-  
detected  
compar-  
le no  
chnique  
loss was  
ted 13 h

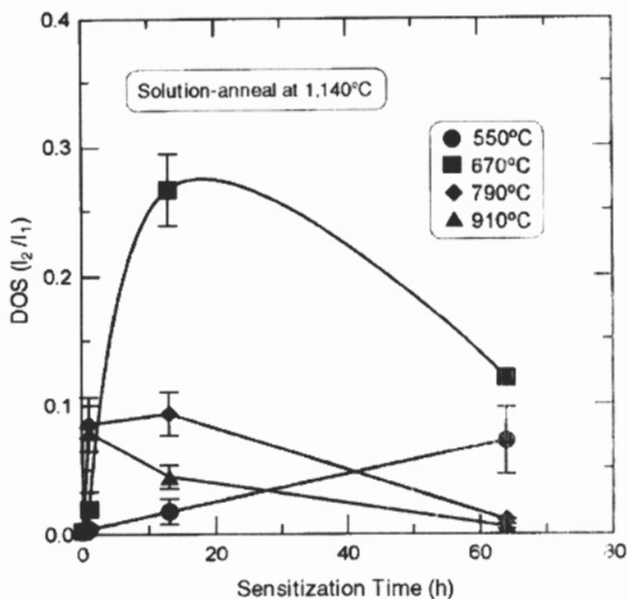


FIGURE 5. DOS variation of Steel 347(2) with sensitization treatment time at different temperatures as determined by the DL-EPR technique.

and 790°C data were practically the same. At other temperatures, agreement was poor. At 550°C and 910°C, weight losses were negligible.

Some of the samples submitted to the Practice B test were examined by scanning electron microscopy (SEM). As-corroded surface morphologies of Steel 347 and Steel 347L samples solution-annealed at 1,050°C presented a large weight loss for 13-h treatment at 670°C and 550°C (Figures 7 and 8). In both cases, corrosion was characterized by the presence of

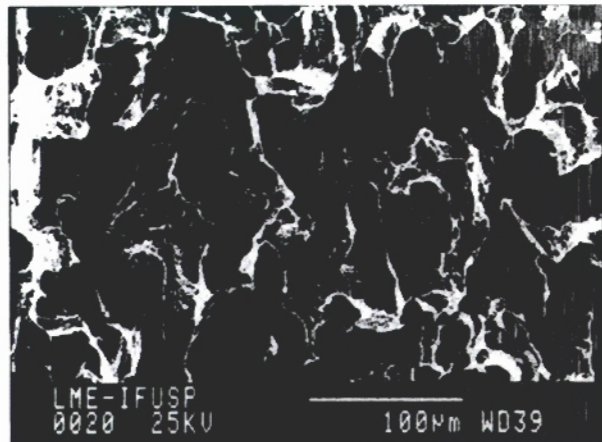


FIGURE 7. As-corroded surface morphology of Steel 347(1) sensitized 13 h at 670°C, after 40 min of immersion in Practice B solution. The deep holes near each other were typical of tunneling corrosion (SEM, 300x).

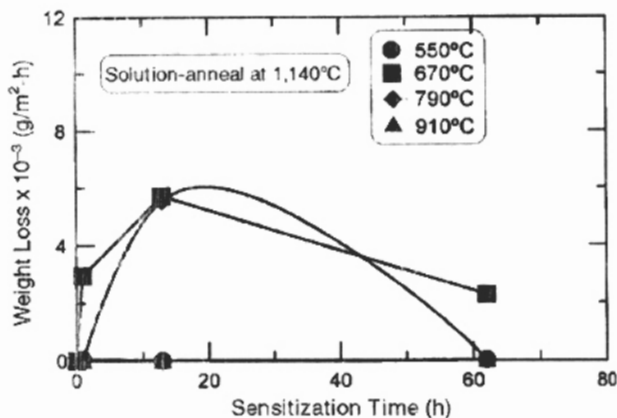


FIGURE 6. Weight-loss variation of Steel 347(2) with sensitization treatment time at different temperatures as determined using ASTM A 262, Practice B, after 30 min of immersion.

deep holes in close proximity, with each hole resembling a corrosion pit. Figure 8 shows these holes as very tunnel-like in shape. Thus, in both cases, this type of attack was typical of tunneling corrosion.

In some samples, intergranular corrosion was observed in addition to tunneling corrosion, as was the case of Steel 347(1) treated for 130 h at 670°C (Figure 9). Intergranular corrosion is shown in more detail in Figure 10. Some intergranular corrosion, although rare, was observed in Steel 347L samples.

For samples solution-annealed at 1,140°C, tunneling corrosion associated with the intergranular corrosion was observed on samples sensitized at 670°C. For samples sensitized at 790°C, corrosion was primarily intergranular, as shown in Figure 11 for the sample sensitized 13 h.

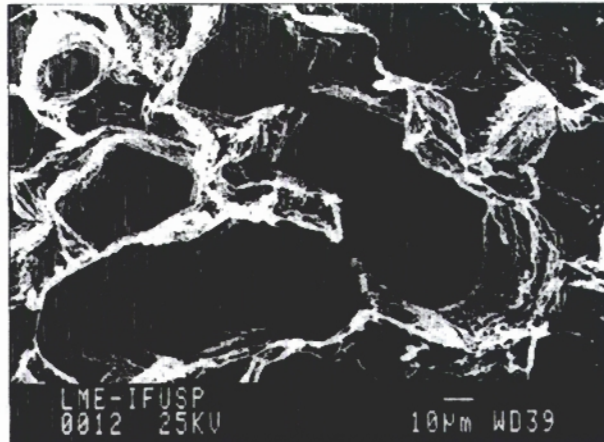


FIGURE 8. As-corroded surface morphology of Steel 347L sensitized 13 h at 550°C, after 40 min of immersion in Practice B solution. The many tunnel-like deep holes, close to each other, were typical of tunneling corrosion (SEM, 600x).

Optical metallography (OM) confirmed the two types of corrosion. Figure 12 shows the tunneling corrosion, and Figure 13 shows the tunneling corrosion associated with some intergranular corrosion. Figure 14 shows intergranular corrosion only.

## DISCUSSION

The behavior of Steel 347(1) (Figure 1) was consistent with Padilha's findings for type 321 SS.<sup>1</sup> Assuming that the same explanations apply to type 347 SS, the carbon retained in solution tended at lower temperatures to combine preferentially with chromium. At higher temperatures, it combined preferentially with niobium, and at intermediate temperatures with both, so that it could be inferred that chromium depletion at grain boundaries was larger at lower than at higher temperatures.

The occurrence of tunneling corrosion in Practice B tests was consistent with findings of Kajimura, et al., and was ascribed to the fact that the samples were made from forged materials.<sup>2</sup> Therefore, the lack of agreement in most cases between the DL-EPR and the Practice B tests seemed to be associated with this type of corrosion. If, as stated by Kajimura, et al., tunneling corrosion is associated with chromium-depleted bands from compositional banding, the DL-EPR test should have been sensitive to these bands, and the sensitization intensity  $I_2/I_1$  ratio should have been larger and should have been in good agreement with the weight loss determined in Practice B tests. However, this did not happen, as clearly shown in Figures 1 and 3 when compared to Figures 2 and 4, respectively.

The possibility of the DL-EPR test being affected by the factors responsible for tunneling corrosion could not be discarded, although it was not clear how this might have happened. According to Kajimura, et al., the areas with chromium depletion could have acted as initiation sites for tunneling corrosion.<sup>2</sup> The tunneling corrosion could have been assisted by other microstructural components, such as stringers of nonmetallic inclusions or segregation of impurity elements such as sulfur or phosphorus. Hence, the DL-EPR test would track the chromium-depleted areas, but the measured amount would not be as large as the weight loss determined in the Practice B test for several reasons. First, the Practice B could be sensitive to smaller levels of chromium depletion than the DL-EPR test. According to Bruemmer, et al., EPR tests register chromium depletion only below ~ 14.5% to 15%.<sup>8</sup> Next, Practice B could be more sensitive to cold work and to the presence of manganese sulfide (MnS) and other nonmetallic inclusions or even ferrite in the structure.

Data of Figure 5 was in good agreement with the temperature-time-corrosion (TTC) curves obtained by Ebling and Sheil for type 347 steel using the weight-

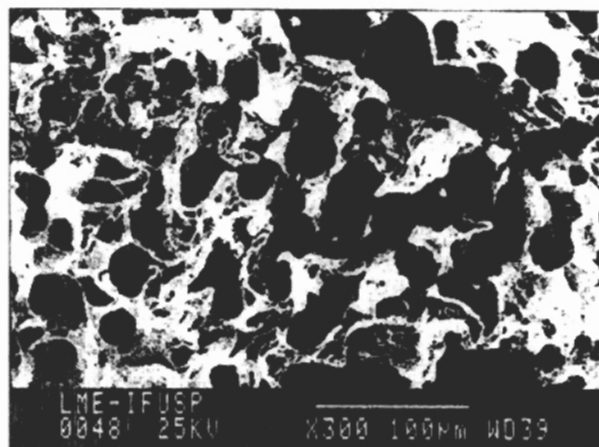


FIGURE 9. As-corroded surface morphology of Steel 347(1) sensitized 130 h at 670°C, after 40 min of immersion in Practice B solution. In addition to tunneling corrosion, some intergranular corrosion was visible in the upper left corner (SEM, 300x).

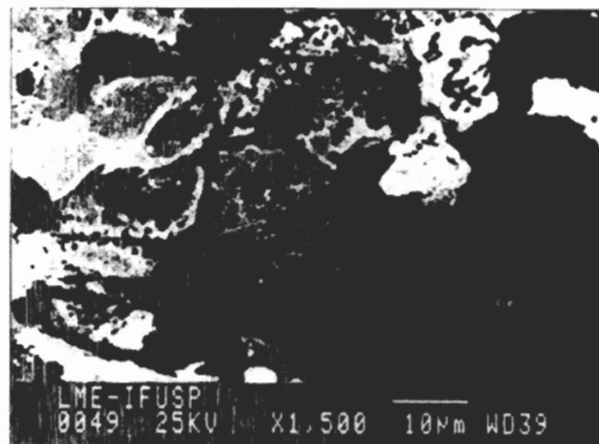


FIGURE 10. Detailed view of intergranular corrosion observed in Figure 9. Cavities suggested detachment of grains (SEM, 1,500x).

loss test in boiling 65% HNO<sub>3</sub>.<sup>9</sup> Figure 15 compares  $I_2/I_1$  values of Figure 5 corresponding to 670°C to the corrosion rate values corresponding to this temperature in the above TTC curves. The two curves were very similar, but the times at which maximum sensitization was reached were different, probably as a result of differences in composition and solution-anneal treatment of the two materials.

By comparing Figure 1 with Figure 5, it was verified that the solution anneal at 1,140°C produced a material more susceptible to sensitization than that at 1,050°C. Reasons for this were related to a larger dissolution of niobium carbides at 1,140°C than at 1,050°C and a larger retention of carbon in solution after the cooling. According to Padilha, et al.,<sup>10</sup> the content [C] (wt%) of carbon dissolved in the matrix of

80

h sensitization  
using ASTM

le resem-  
: holes as  
ises, this  
rosion.  
ion was  
n, as was  
it 670°C  
m in more  
rosion,  
samples.  
10°C, tun-  
granular  
ized at  
orrosion  
Figure 11



347L sensitized  
B solution. The  
were typical of



**FIGURE 11.** As-corroded surface morphology of Steel 347(2) sensitized 13 h at 790°C, after 30 min of immersion in Practice B testing solution. Corrosion was primarily intergranular (SEM, 300x).

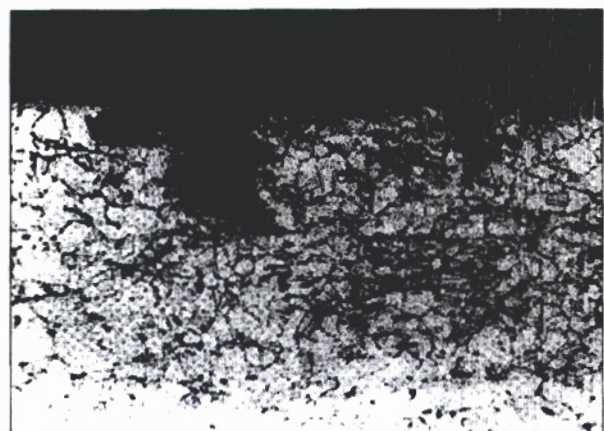


**FIGURE 13.** Tunneling corrosion and some intergranular corrosion of Steel 347(2) sensitized 13 h at 670°C, after 30 min of immersion in Practice B testing solution (OM, etched with oxalic acid, 150x).

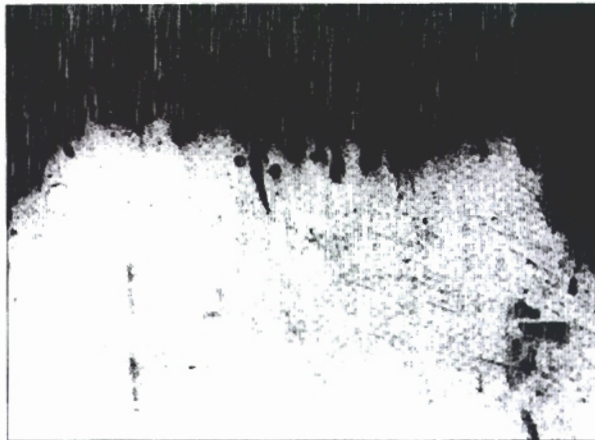


**FIGURE 12.** Tunneling corrosion of Steel 347L sensitized 13 h at 550°C, after 40 min of immersion in Practice B testing solution (OM, etched with oxalic acid, 150x).

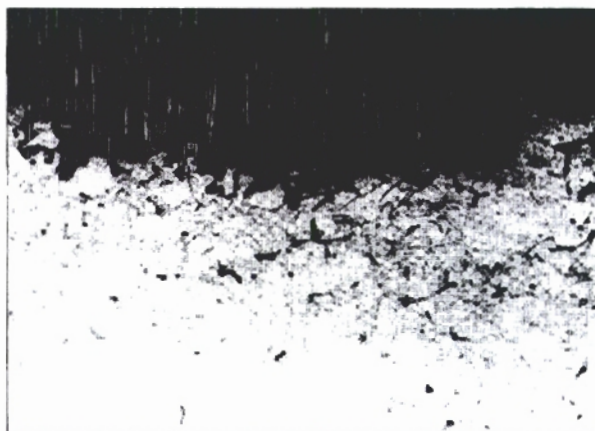


**FIGURE 14.** Intergranular corrosion of Steel 347(2) steel sensitized 13 h at 790°C, after 30 min of immersion in Practice B testing solution (OM, etched with oxalic acid, 150x).

an austenitic SS due to the dissolution of a given metallic carbide is given by:

$$a[C]^2 - (ac - b)[C] - 10^d = 0 \quad (1)$$

where  $a$  is the stoichiometric ratio of metal to the carbon in the carbide,  $b$  is the total wt% of carbide forming metal in steel,  $c$  is the total wt% of carbon in steel, and  $d = \log [M][C]$ , with  $[M]$  being the wt% of the carbide-forming metal dissolved in the matrix. For NbC, the  $d$  value for 18% Cr-13% Ni steel in the range 1,000°C to 1,300°C changes with temperature as:<sup>11</sup>

$$d = 4.55 - \frac{9,350}{T} \quad (2)$$

Applying these equations to the investigated Steel 347, for which  $b$  was assumed to be 0.76% (the tantalum content is usually very small) and  $c = 0.064\%$ , the carbon content  $[C]$  in solution was 0.0092% at 1,050°C and 0.020% at 1,140°C, which confirmed the above assumption.

Chromium carbide precipitation in Steel 347(2) at temperatures  $> 600^\circ\text{C}$  was determined certainly by the larger carbon availability in solution. This also could have been affected by the smaller density of niobium carbides due to their dissolution at 1,140°C. The undissolved niobium carbides would act as pre-existing nuclei for carbon precipitation as NbC, and if there were few, the chromium carbide precipitation would be stimulated. However, the participation of these preexisting nuclei in NbC nucleation apparently was not very significant, and there was no data

available nuclei is

In a whose same section curves balance kinetics depleted the chromium could be Figure 5 when the 910°C. H diffusion zones, w ture, res decrease

From carbide p the slope This see 670°C, a first point times in Assuming approxi curves re Arrheniu trapolat to the te be of ~ 0, example, 8 min). T chromium was cons occurred

The i good as t sible that corrosion and 670° corrosion zones,<sup>2</sup> a measur increase the point Justed st corrosion position (

From possible chromium boundaries than that It was po caused by be small

available showing how the number density of these nuclei is affected by the solution-anneal temperature.

In a similar way to type 304 SS (UNS S30400), whose sensitization kinetics was investigated by the same technique,<sup>12</sup> it could be stated that sensitization curves, such as those of Figure 5, result from a balance between the chromium carbide precipitation kinetics and the kinetics by which the chromium-depleted zones are eliminated by diffusion. Indeed, the chromium carbide precipitation kinetics, which could be associated with the slopes of the curves of Figure 5 for small sensitization times, increased when the temperature increased from 550°C to 910°C. However, there was a simultaneous "back" diffusion of chromium to the chromium-depleted zones, whose kinetics also increased with temperature, resulting in a gradual stabilization and a decrease of DOS for longer sensitization times.

From the above considerations, the chromium carbide precipitation rate could be estimated from the slope of the tangent to these curves at the origin. This seemed to be valid for temperatures of 550°C, 670°C, and 790°C, but not for 910°C, for which the first point of the curve, that of 1 h, was already at times in which chromium diffusion was dominant. Assuming this evaluation was valid and using the approximate values of the slopes at the origin of the curves related to 550°C, 670°C, and 790°C, the Arrhenius plot of Figure 16 was obtained. The extrapolation of the straight line fitted to these points to the temperature at 910°C indicated its slope would be of ~0.34 (i.e., the time necessary to reach, for example, DOS of  $I_2/I_1 = 0.05$ , would be of the order of 8 min). This value, associated to a considerably high chromium diffusion coefficient at this temperature, was consistent with the sensitization decrease that occurred between 1 h and 13 h.

The alignment of points in Figure 16 was not as good as that reported for type 304 SS.<sup>12</sup> It was possible that the reason for this was the tunneling corrosion observed on samples sensitized at 550°C and 670°C. As stated by Kajimura, et al., this type of corrosion is determined by chromium-depleted zones,<sup>2</sup> and it is quite possible that in the DL-EPR measuring technique, these zones contributed to the increase of the  $I_2/I_1$  ratio. This should explain why the point corresponding to 670°C was above the adjusted straight line, while the absence of tunneling corrosion in samples sensitized at 790°C justified the position of the corresponding point below this line.

From the slope of Arrhenius straight line, it was possible to determine the activation energy of the chromium carbide precipitation rate at the grain boundaries as 124 kJ/mol. This value was larger than that determined for type 304 SS (103 kJ/mol).<sup>12</sup> It was possible that, with the exclusion of the effect caused by the tunneling corrosion, this value would be smaller and closer to that of type 304 SS.

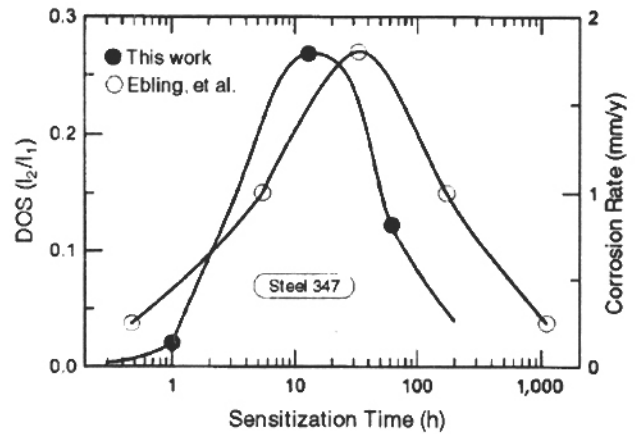


FIGURE 15. DOS variation with sensitization time obtained by the DL-EPR technique for Steel 347 solution-annealed at 1,140°C and sensitized at 670°C, compared to that obtained by Ebling and Scheiff using the weight-loss test in boiling 65% HNO<sub>3</sub>.

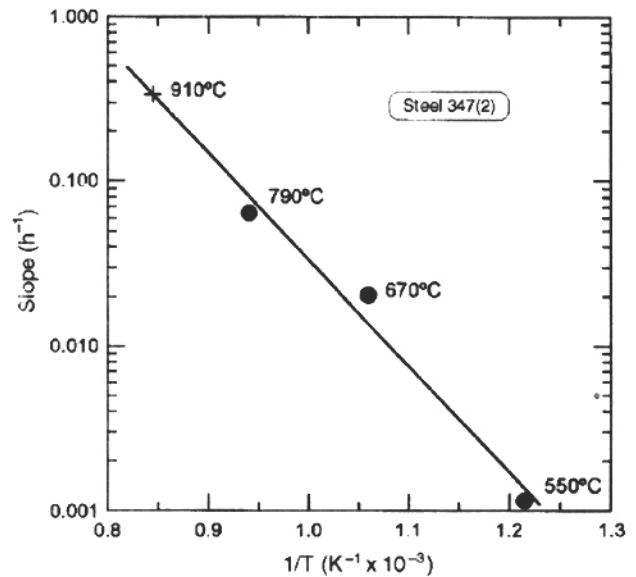


FIGURE 16. Arrhenius plot for the tangent slopes at the origin of the curves of Figure 5, determined for 550°C, 670°C, and 790°C, and extrapolated to 910°C.

Finally, in some cases, the weight loss determined by Practice B was negligible while the sensitization intensity  $I_2/I_1$  as determined by the DL-EPR test was substantial (for instance, the sample sensitized at 550°C in Figures 3 and 4). The reason for this may have been the short time adopted for the immersion test (only 40 min). Dissolution of the metal only started when the passive film of chromium-depleted areas was broken. This film breakdown was a probabilistic phenomenon and involved an induction period, which may have varied

from one test to another. Thus, it was possible that, for some samples, this induction period was not reached during the adopted testing time.

## CONCLUSIONS

- ◆ Tunneling corrosion observed on Steel 347 and Steel 347L samples submitted to the ASTM A 262, Practice B test was related to their forging microstructure, although it was not clear what factors actually were controlling.
- ◆ The DL-EPR test seemed mostly sensitive to the intergranular corrosion determined by sensitization, while the Practice B test did not discriminate between this type of attack and that of tunneling corrosion. This implied that the results of Practice B, when applied to forged SS, must be used with discretion, because an expressive weight loss will not necessarily mean that the material is sensitized.
- ◆ The solution-annealing of Steel 347 at 1,140°C produced a material more susceptible to sensitization than that at 1,050°C because more carbon remained in solution in the former.
- ◆ The points in the Arrhenius diagram, corresponding to the chromium carbide precipitation kinetics at grain boundaries of the investigated steel, were not aligned perfectly probably because of the simultaneous occurrence of tunneling corrosion. The activation energy of this process was 124 kJ/mol, which was slightly higher than that determined for type 304 SS.

## ACKNOWLEDGMENTS

The authors acknowledge a scholarship for C.A. Teodoro from the Brazilian Bureau for Development of Personnel with Higher Education (CAPES) and the Brazilian National Council for Scientific and Techno-

logical Development (CNPq) and financial support for the research from the Foundation for Research Support of the State of São Paulo (FAPESP).

## REFERENCES

1. A.F. Padilha, "Precipitation Behavior of Titanium-Stabilized 15% Cr-15% Ni-1% Mo-Ti-B Austenitic Stainless Steels" (Ph.D. thesis, Universität Karlsruhe, Germany, 1981, in German).
2. H. Kajimura, M. Harada, T. Okada, M. Okubo, N. Nagano, *Corrosion* 51, 7 (1995): p. 507.
3. R.D. Shaw, D. Elliott, "Stainless Steels in U.K. Nuclear Fuel Reprocessing Plants," *Proc. Stainless Steel '84*, September 1984, Goteborg, Sweden (London, England: The Institute of Metals, 1985), p. 395.
4. U. Blom, B. Kvamback, *MP* 14, 7 (1975): p. 43.
5. C.A. Teodoro, S. Wolyneec, "Sensitization Kinetics Investigation of AISI 304, 374, and 347L Stainless Steels Using the Potentiokinetic Reactivation Technique," *Proc. 12th Brazilian Cong. Materials Engineering and Science*, December 1994, vol. 1 (São Paulo, Brazil: EPUSP, Polytechnic School of University of São Paulo, 1994), p. 335 (in Portuguese).
6. A.P. Majidi, M.A. Streicher, *Nucl. Technol.* 75 (1986): p. 356.
7. S.B. Faldini, S. Wolyneec, "Influence of Stirring in Electrochemical Potentiokinetic Reactivation Test for Sensitization Determination of Austenitic Stainless Steels," *Proc. 7th Brazilian Symp. Electrochemistry and Electroanalysis*, April 1990, vol. 1 (Ribeirão Preto, Brazil: University of São Paulo, 1990), p. 93 (in Portuguese).
8. S.M. Bruemmer, L.A. Charlot, B.W. Arey, *Corrosion* 44, 6 (1988): p. 328.
9. H.F. Ebling, M.A. Scheil, as cited by M. Henthorne, "Intergranular Corrosion in Iron- and Nickel-Based Alloys," in *Localized Corrosion: Cause of Metal Failure*, ASTM STP 516 (Philadelphia, PA: ASTM, 1972), p. 66.
10. A.F. Padilha, J.C. Petoilho, I.G.S. Falleiros, "Discussion of the Effects of Zr, Ti, Nb, and V Additions Upon Austenitic Stainless Steels Microstructure," *Proc. Seminar on Physical Metallurgy and Heat Treatments*, 1983 (São Paulo, Brazil: ABM, Brazilian Society for Metals, 1983), p. 93 (in Portuguese).
11. S.R. Keown, F.B. Pickering, "Effect of Niobium Carbides on Creep Rupture Properties of Austenitic Stainless Steels," *Proc. Conf. on Creep Strength in Steel and High-Temperature Alloys*, September 1972, Sheffield, England (London, England: The Metals Soc., 1974), p. 134.
12. C.A. Teodoro, S. Wolyneec, "Sensitization Kinetics Investigation of AISI 304 Austenitic Stainless Steel Using the Potentiokinetic Reactivation Technique," paper no. LA 96093, *Proc. 2nd NACE Latin American Region Corrosion Congress*, 1996 (Rio de Janeiro, Brazil: Goal Promoções e Feiras, 1996).

Roll  
Beh

O.P. Mo

ABSTR

Observa  
alloys de  
were an  
sodium c  
potentio  
subjecte  
ence of t  
composit  
matrix a  
disperso  
found to  
Results  
observat

KEY WO  
graphite  
silicon c

INTRO

It has b  
with gr  
rior cor  
alloys i  
variable  
matrix  
nature  
sold/m  
therein

Subm  
1997.  
• Region  
• UNS n  
Numb  
Engin

1997  
Author's  
Guide\*



Now Available  
by Fax or the Internet!

# THE JOURNAL OF SCIENCE AND ENGINEERING CORROSION

A free 16-page guide for the prospective *CORROSION* author, with tips on manuscript preparation, format, style, color artwork, and editorial policies.

To order, contact: NACE Membership Services Department, P.O. Box 218340, Houston, TX, 77218-8340; Phone: 281/228-6223, or Fax 281/228-6329; ask for Item no. 32143. For immediate delivery by fax, call 1-800-593-2735 in the United States, or 214-353-6134 elsewhere. Also available on the NACE web page at [www.nace.org](http://www.nace.org).